

DESI 2024: Reconstructing Dark Energy using Crossing Statistics with DESI DR1 BAO data

R. Calderon¹, K. Lodha^{1,2}, A. Shafieloo^{1,2}, E. Linder^{3,4,5},
W. Sohn¹, A. de Mattia⁶, J. L. Cervantes-Cota⁷, R. Crittenden,⁸
T. M. Davis⁹, M. Ishak¹⁰, A. G. Kim³, W. Matthewson,¹
G. Niz^{11,12}, S. Park^{1,2}, J. Aguilar,³ S. Ahlen¹³, S. Allen,^{14,15}
D. Brooks,¹⁶ T. Claybaugh,³ A. de la Macorra¹⁷, A. Dey¹⁸,
B. Dey¹⁹, P. Doel,¹⁶ J. E. Forero-Romero^{20,21},
E. Gaztañaga,^{22,8,23} S. Gontcho A Gontcho³, K. Honscheid,^{24,25,26}
C. Howlett⁹, S. Juneau,¹⁸ A. Kremin³, M. Landriau³,
L. Le Guillou²⁷, M. E. Levi³, M. Manera^{28,29}, R. Miquel,^{30,29}
J. Moustakas³¹, J. A. Newman¹⁹, N. Palanque-Desabrouille^{6,3},
W. J. Percival^{32,33,34}, C. Poppett,^{3,4,5} F. Prada³⁵, M. Rezaie³⁶,
G. Rossi,³⁷ V. Ruhlmann-Kleider⁶, E. Sanchez³⁸, D. Schlegel,³
M. Schubnell,^{39,40} H. Seo⁴¹, D. Sprayberry,¹⁸ G. Tarlé⁴⁰,
P. Taylor,²⁶ M. Vargas-Magaña¹⁷, B. A. Weaver,¹⁸ P. Zarrouk²⁷,
H. Zou⁴²

Affiliations are in Appendix F

E-mail: calderon@kasi.re.kr, shafieloo@kasi.re.kr

Abstract. We implement Crossing Statistics to reconstruct in a model-agnostic manner the expansion history of the universe and properties of dark energy, using DESI Data Release 1 (DR1) BAO data in combination with one of three different supernova compilations (PantheonPlus, Union3, and DES-SN5YR) and Planck CMB observations. Our results hint towards an evolving and emergent dark energy behaviour, with negligible presence of dark energy at $z \gtrsim 1$, at varying significance depending on data sets combined. In all these reconstructions, the cosmological constant lies outside the 95% confidence intervals for some redshift ranges. This dark energy behaviour, reconstructed using Crossing Statistics, is in agreement with results from the conventional w_0-w_a dark energy equation of state parametrization reported in the DESI Key cosmology paper. Our results add an extensive class of model-agnostic reconstructions with acceptable fits to the data, including models where cosmic acceleration slows down at low redshifts. We also report constraints on $H_0 r_d$ from our model-agnostic analysis, independent of the pre-recombination physics.

Contents

1	Introduction	1
2	Methodology and Data	2
2.1	Crossing Statistics	2
2.2	Dark energy modeling	3
2.2.1	Equation of state	3
2.2.2	Dark energy density	4
2.3	Data	4
2.4	Analysis	5
3	Results	6
3.1	Results using $w(z)$	6
3.2	Results using $f_{\text{DE}}(z)$	9
4	Discussion and Conclusions	11
A	Order of the Chebyshev expansion	14
B	Robustness of z_{max}	14
C	Crossing hyperparameters and effect of priors	16
D	Comparison with (DESI+SDSS)	16
E	Comparison with w_0w_aCDM	16
F	Author Affiliations	24

1 Introduction

The concordance model of cosmology, rooted in Einstein’s general theory of relativity (GR), provides a testable and falsifiable theory of the Universe. As an isotropic and homogeneous universe, with standard model radiation and matter, plus cold dark matter and a cosmological constant, the concordance Λ CDM model has proved to be highly successful in explaining the wide array of cosmological observations [1–5]. This predictive model effectively describes the Universe’s dynamics with only 6 free parameters. However, cosmic acceleration has such fundamental implications, that a key aim in physical cosmology has been to challenge the assumption that dark energy is synonymous with the cosmological constant [6–12], a query central to many cosmological surveys and instruments [13–18]. Many cosmologists have aimed to reconstruct the expansion history of the universe and understand the properties of dark energy, leading to the introduction of numerous parametric and nonparametric approaches [19–35].

In this study, we employ the technique of Crossing Statistics [36, 37] on DESI BAO data, combined with supernovae and CMB data, to reconstruct the expansion history of the universe and properties of dark energy. Crossing Statistics serve to assess deviations from an

assumed background model (in this case, the cosmological constant as dark energy) and offer a wide range of viable reconstructions tailored to different data combinations. Our findings suggest that the data combination is consistent with, and to some extent in favor of, an evolving emergent behaviour of dark energy with a slowing down of the acceleration at low redshifts.

2 Methodology and Data

In this paper, we use the most recent Baryon Acoustic Oscillations (BAO) observations from the Dark Energy Spectroscopic Instrument (DESI) along with different supernova compilations and cosmic microwave background data. Here we briefly explain the methods and data we use in this analysis.

2.1 Crossing Statistics

Crossing Statistics were originally introduced to extract information from data beyond the conventional χ^2 statistics and its relation to likelihoods. With the median statistic as its first mode and the χ^2 statistic as its last mode, Crossing Statistics can be considered as a generalization of χ^2 statistics [38]. While the original Crossing Statistics are hard to implement for the purpose of model validation, model selection, and parameter estimation, their Bayesian interpretation can be trivially used for such purposes [36, 37]. Crossing Statistics can also be used in some other contexts, including reconstruction and consistency tests [39–41, see also [42] for the use of Chebyshev polynomials for reconstruction.].

In this work, we use the Crossing Statistic formalism for the reconstruction of the dark energy properties [36, 37]. In particular, we use the fact that any given function $y(z)$ can be expanded as a Chebyshev series

$$y(z) = \sum_{i=0}^N C_i T_i(x), \quad x \equiv 1 - 2 \frac{z_{\max} - z}{z_{\max} - z_{\min}} \in [-1, 1], \quad (2.1)$$

where $T_i(x)$ are the Chebyshev polynomials of the first kind, defined in the interval $x \in [-1, 1]$, and C_i are some coefficients multiplying these polynomials. The Chebyshev polynomials, in the limit $N \rightarrow \infty$, form a basis that spans the space of all continuous functions. For practical purposes, we limit the analysis to four terms in the expansion; including higher orders leads to weaker constraints, due to the increased number of degrees of freedom¹. In [Appendix A](#) we provide further motivations for this choice. The first four Chebyshev polynomials are given by

$$\begin{aligned} T_0(x) &= 1, & T_1(x) &= x, \\ T_2(x) &= 2x^2 - 1, & T_3(x) &= 4x^3 - 3x. \end{aligned} \quad (2.2)$$

We use these polynomials to model the energy density and equation of state of dark energy and to reconstruct its possible time-dependence from the data, as described in [Section 2.2](#) below. We choose $z_{\min} = 0$ and $z_{\max} = 3.5$, beyond which redshift there are no more data to constrain its evolution. See the individual subsections below regarding $z > z_{\max}$. We

¹In practice, the maximum order of polynomials should be set as the smallest integer compatible with the data. Previous works have shown that using up to four terms of Crossing Statistics is generally sufficient to capture the time evolution of smooth functions in a limited range [36, 39].

have verified that the results do not differ significantly if instead we choose $z_{\max} = 2.35$ (see [Appendix B](#)). Note that many stage 4 surveys will probe physics at $z \lesssim 3.5$ [[43–46](#)]. Also note that unlike previous analyses using crossing statistics [[39–41](#)], where $x \in [0, 1]$ was used, we use the full range $x \in [-1, 1]$ spanned by the polynomials (cf. [Eq. \(2.1\)](#)).

In the Bayesian interpretation of the crossing statistic [[37](#)], the posterior distribution of the Chebyshev coefficients C_i carries valuable information on the model (mean function) at hand. Any significant deviation from the mean function C_i 's would indicate that the data favors deformations away from the considered model (see [Appendix C](#)).

2.2 Dark energy modeling

Assuming a flat universe, the Friedmann equation reads

$$\frac{H^2(z)}{H_0^2} = \Omega_{\text{m},0}(1+z)^3 + \Omega_{\text{r},0}(1+z)^4 + (1 - \Omega_{\text{m},0} - \Omega_{\text{r},0}) f_{\text{DE}}(z) \quad (2.3)$$

where $\Omega_{i,0} \equiv 8\pi G\rho_i/3H_0^2$ are the fractional energy density parameters of the respective components at the present time and $f_{\text{DE}}(z) \equiv \rho_{\text{DE}}(z)/\rho_{\text{DE},0}$ is the effective (normalized) dark energy density, which accounts for any additional contribution to the expansion rate coming from e.g. unknown energy density or modified gravity. Using the conservation of energy, the energy density can be related to the pressure to energy density ratio of dark energy through its equation of state parameter $w(z)$,

$$f_{\text{DE}}(z) \equiv \frac{\rho_{\text{DE}}(z)}{\rho_{\text{DE},0}} = \exp\left(3 \int_0^z [1 + w(\tilde{z})] \, \text{d} \ln(1 + \tilde{z})\right). \quad (2.4)$$

A common approach used to explore alternative dark energy models is to parameterize the time evolution of its equation of state. The standard parametrization, $w(a) = w_0 + w_a(1-a)$ [[47, 48](#)], has been shown to be highly accurate for a wide variety of models [[48, 49](#)].

Alternatively, a bottom-up approach involves reconstructing its redshift evolution directly from the data using non-parametric methods (see for example [[19, 20, 25, 27, 28, 30–35, 50–56](#)]). In this work, we explore an extended reconstruction for dark energy, both in terms of its equation of state and its energy density to see if the data suggest more complicated dynamics.

2.2.1 Equation of state

We start by exploring a flexible parameterization for the equation of state, $w(z)$. We use the Chebyshev expansion in [Eq. \(2.1\)](#) with four terms, around $w = -1$,

$$w(z) = -1 \times \sum_{i=0}^{N=3} C_i T_i(x). \quad (2.5)$$

This parametrization introduces four additional degrees of freedom, captured by the four coefficients C_i multiplying the polynomials given by [Eq. \(2.2\)](#). For moderate redshift (geometrical) probes, such as BAO and SN, we compute distances and constrain the energy content of our models, treating the degenerate combination $H_0 r_{\text{d}}$ as a free parameter. We

will refer to this as “background-only”. When including the measurements from the cosmic microwave background, we implement this parametrization using our modified version of the Boltzmann solver `class` [57, 58] that allows for an arbitrary redshift dependence of $w(z)$. In order that we give enough flexibility to the dark energy behaviour at low redshifts (where dark energy is most dominant) —and to be consistent with our “background-only” runs —beyond $z_{\text{max}} = 3.5$ we smoothly extrapolate the equation of state $w(z)$ to a cosmological constant $w = -1$ using a transition function $-1 + (B_0 + B_1 \cdot u)e^{-u^2/\Delta^2}$ where $u = \log \frac{1+z}{1+z_{\text{max}}}$, and B_0, B_1 are chosen to ensure $w(z)$ remains smooth and differentiable at the transition. Unlike [59], we give more freedom to the equation of state, focusing on the very low- z regime and using the whole range spanned by the polynomials, whereas a very broad $x = \log(1+z)/\log(1+z_{\text{rec}})$ was used in [59]. To allow for a phantom equation of state, $w(z) < -1$, we rely on the Parametrized-Post Friedmann (PPF) framework [60], as implemented in `class`. Moreover, our main focus being the geometrical probes, all the runs in this analysis assume a sound speed $c_s^2 = 1$ for the dark energy fluid. Including dark energy perturbations is beyond the scope of this work. We present our findings, using both the “background-only” probes and those including the CMB, in Section 3.1.

2.2.2 Dark energy density

Alternatively to the equation of state, one can directly reconstruct the redshift dependence of the dark energy density. The main advantage of working with the effective energy density, $\rho_{\text{DE}}^{\text{eff}}(z)$, is that it allows us to cover a larger class of models. Unlike the equation of state parameter $w(z)$, the direct reconstruction of $f_{\text{DE}}(z)$ allows for the effective energy density to become negative, which can happen in modified gravity [61–65] and various other dark energy models [66–73]. The normalized energy density evolution f_{DE} is then written as

$$f_{\text{DE}}(z) = C_0 + \sum_{i=1}^{N=3} C_i T_i(x) . \quad (2.6)$$

The function f_{DE} , defined in Eq. (2.4), satisfies by definition $f_{\text{DE}}(z=0) \equiv 1$. Thus, C_0 is not a free-parameter and must be determined for each $C_{i>0}$ using the closure relation

$$C_0 = 1 - \sum_{i=1}^{N=3} C_i T_i(x=-1) = 1 - \sum_{i=1}^{N=3} C_i \times (-1)^i . \quad (2.7)$$

Note that a cosmological constant ($f_{\text{DE}} = 1$) is recovered for $C_0 = 1, C_{i>0} = 0$. Due to complications arising from the treatment of perturbations with negative energy densities, we restrict this part of the analysis to the “background-only” probes, and so always $z < z_{\text{max}}$. The results when directly reconstructing $f_{\text{DE}}(z)$ are presented in Section 3.2.

2.3 Data

- **Baryon Acoustic Oscillations (BAO):** We use the compilation of compressed distance quantities D_{M}/r_d , D_{H}/r_d , and D_{V}/r_d from the first year data release (DR1) of the Dark Energy Spectroscopic Instrument (DESI) [18, 74–77], as given in [78]. BAO measures effective distances relative to the drag-epoch sound horizon $r_d \equiv r_s(z_{\text{drag}})$. Along the line of sight we measure

$$\frac{D_{\text{H}}(z)}{r_d} \equiv \frac{c}{H(z)r_d} = \frac{c}{H_0 r_d} \frac{1}{h(z)} , \quad (2.8)$$

where $h(z) = H(z)/H_0$, and transverse to the line of sight we measure

$$\frac{D_M(z)}{r_d} \equiv \frac{c}{r_d} \int_0^z \frac{d\tilde{z}}{H(\tilde{z})} = \frac{c}{H_0 r_d} \int_0^z \frac{d\tilde{z}}{h(\tilde{z})}, \quad (2.9)$$

while $D_V \equiv [z D_M^2(z) D_H(z)]^{1/3}$ is an angle-averaged effective ‘‘monopole’’ distance. This dataset, abbreviated as ‘‘DESI BAO’’, spans seven redshift bins from $z = 0.3$ to $z = 2.33$ (where the last bin extends out to $z \approx 3.5$) [79]. Additionally, in some cases (see Appendix D) we use the combination of DESI and SDSS data, referred to as ‘‘(DESI+SDSS) BAO’’, taking the three redshift bins at $z < 0.6$ from SDSS with tighter constraints, while keeping DESI results for $z > 0.6$. For Ly α data, we employ the combined DESI+SDSS results provided by [80]. We direct the reader to [18, 78–83] for further details on these data sets and BAO combination choices.

- **Supernovae Ia (SNe Ia):** For some combined data sets we use supernova data from three compilations, one at a time: ‘‘PantheonPlus’’, a compilation of 1550 supernovae spanning 0.01 to 2.26 [84]; ‘‘Union3’’, containing 2087 SNe Ia processed through the Unity 1.5 pipeline based on Bayesian Hierarchical Modelling [85]; and ‘‘DES-SN5YR’’, a compilation of 194 low-redshift SNe Ia ($0.025 < z < 0.1$) and 1635 photometrically classified SNe Ia covering the range $0.1 < z < 1.3$ [86]. SNe Ia give measures of luminosity distances $D_L(z) = (1+z) D_M(z)$.
- **Cosmic Microwave Background (CMB):** We also include temperature and polarisation measurements of the CMB from the Planck satellite [87]. In particular, we use the high- ℓ TTTEEE likelihood (`planck_2018_highl_plik.TTEEE`), together with low- ℓ TT (`planck_2018_lowl.TT`) and low- ℓ EE (`planck_2018_lowl.EE`) [88], as implemented in `cobaya` [89].

2.4 Analysis

We perform an MCMC sampling of the parameter space using the Metropolis-Hastings [90, 91] algorithm implemented in the publicly available sampler `cobaya` [89]. The priors used in the analysis are given in Table 1. When considering non-CMB observations (i.e. SNe and BAO), we use a custom theory code inheriting from `cobaya`’s `Theory` base class to compute the observables (i.e. distances). This only requires the knowledge of the background expansion history (as implemented in Eq. (2.3) above). For such cases, we sample $\vec{\theta} = \{\Omega_{m,0}, C_0, C_1, C_2, C_3, H_0 r_d\}$, where the C_i ’s determine the dark energy behaviour and we treat the combination $H_0 r_d$ as a nuisance parameter. When including the CMB likelihood, we use our modified version of the Boltzmann solver `class` to implement a custom equation of state for dark energy. In that case, the parameter space associated with our model is $\vec{\theta} = \{\omega_{\text{cdm}}, \omega_{\text{b}}, \ln(10^{10} A_s), n_s, \tau, H_0, C_0, C_1, C_2, C_3\}$ where r_d is no longer a free parameter, but its value is rather derived assuming standard pre-recombination physics. Throughout this work, we assume two massless and one massive neutrino, with $m_\nu = 0.06$ eV. We take advantage of the ‘‘fast-dragging’’ scheme [92] when sampling the CMB Planck likelihoods. For the PantheonPlus, DES-SN5YR and Union3 likelihoods, the marginalization over the absolute magnitude M_B is done analytically. The details of the dark energy modelling and its numerical implementation are given in Section 2.2.

One important thing to mention at this point is the choice of prior for the Chebyshev coefficients C_i ’s (or hyperparameters). Similar to what happens in many other analyses, having no ‘‘physically-motivated’’ priors for the C_i ’s can lead to prior-volume effects that could

Table 1. Parameters and priors used in the analysis. All of the priors are uniform in the ranges specified below, except for the hyperparameters C_i where we used a Gaussian prior centered around the mean $\mu^{\Lambda\text{CDM}}$ ($C_0 = 1$, $C_{i>0} = 0$). We consider two sets of parameters, “background-only” when using BAO and SNe data only, and “CMB” where our modified version of the Boltzmann solver `class` has been used.

	parameter	prior/value
background-only	$\Omega_{\text{m},0}$	$\mathcal{U}[0.01, 0.99]$
	$H_0 r_{\text{d}} [\text{km s}^{-1}]$	$\mathcal{U}[3650, 18250]$
CMB	$\omega_{\text{cdm}} \equiv \Omega_{\text{cdm}} h^2$	$\mathcal{U}[0.001, 0.99]$
	$\omega_{\text{b}} \equiv \Omega_{\text{b}} h^2$	$\mathcal{U}[0.005, 0.1]$
	$\ln(10^{10} A_s)$	$\mathcal{U}[1.61, 3.91]$
	n_s	$\mathcal{U}[0.8, 1.2]$
	$H_0 [\text{km s}^{-1} \text{Mpc}^{-1}]$	$\mathcal{U}[20, 100]$
	τ	$\mathcal{U}[0.01, 0.8]$
Hyperparameters	$C_{i=0,1,2,3}^w$	$\mathcal{N}(\mu^{\Lambda\text{CDM}}, \sigma = 3)$
	$C_{i=0,1,2,3}^{f_{\text{DE}}}$	$\mathcal{N}(\mu^{\Lambda\text{CDM}}, \sigma = 1)$

potentially bias the results, as explained in [Appendix C](#). To prevent this from happening, we give Gaussian priors on $C_i \sim \mathcal{N}(\mu^{\Lambda\text{CDM}}, \sigma^2)$, where $\mu^{\Lambda\text{CDM}}$ correspond to the point $C_0 = 1$ and $C_{i>0} = 0$. This ensures that any significant deviation from the mean function (ΛCDM) is purely driven by the data.

3 Results

In this section, we present our findings using different data combinations and compare the reconstructions when using crossing statistics on the equation of state $w(z)$, or the energy density $f_{\text{DE}}(z)$.

3.1 Results using $w(z)$

We start by discussing the results when treating the dark energy equation of state parameter $w(z)$ as a Chebyshev series up to four terms. In the top panels of [Fig. 1](#), we show the redshift evolution of the equation of state, $w(z)$, while the second row shows its corresponding effective dark energy density, $f_{\text{DE}}(z)$, for various data combinations. The third row shows the constraints on the shape of the expansion history, $h(z) = H(z)/H_0$, normalized to the best fit ΛCDM model for visual clarity. In the fourth row, we show the corresponding $Om(z)$ diagnostic. The $Om(z)$ diagnostic [[93](#)] was specifically tailored to efficiently distinguish dark energy models from a cosmological constant, and is defined as

$$Om(z) \equiv \frac{h^2(z) - 1}{(1+z)^3 - 1}. \quad (3.1)$$

For ΛCDM one has simply $Om(z) = \Omega_{\text{m},0}$. Finally, in the bottom panel, we also plot the evolution of the deceleration parameter $q(z)$, defined as

$$q(z) \equiv -\frac{\ddot{a}a}{\dot{a}^2} = -\frac{\dot{H}}{H^2} - 1 = \frac{d \ln H}{d \ln(1+z)} - 1. \quad (3.2)$$

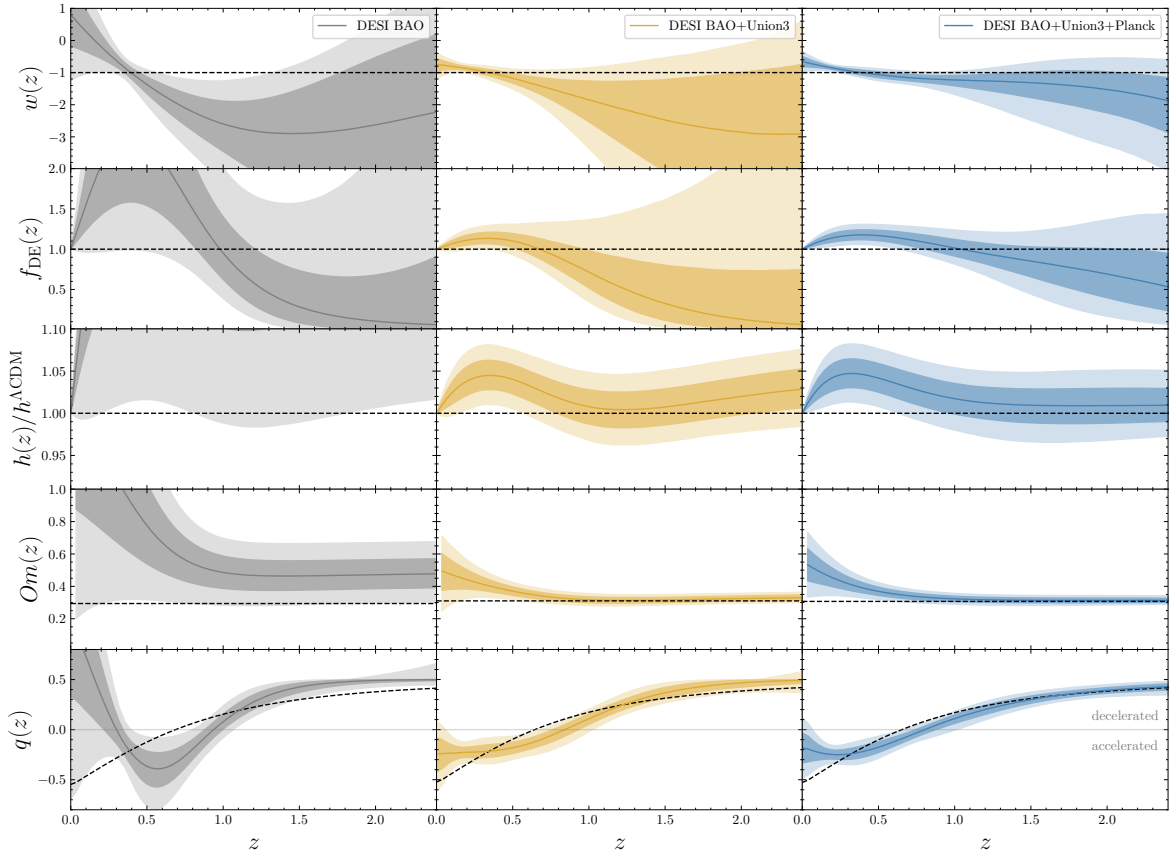


Figure 1. Dark energy reconstructions using the Chebyshev expansion of $w(z)$ up to four terms with DESI BAO, DESI BAO+Union3, and DESI BAO+Union3+Planck datasets, respectively. The colored lines correspond to the median of the posterior distributions and the shaded regions show the 68% and 95% confidence intervals around it. The black-dashed lines depict the best-fit Λ CDM predictions for each data combination.

In all cases, the dashed black lines represent the Λ CDM best-fit values for these quantities, and for each data combination. The coloured lines correspond to the median of the posterior distributions and the shaded regions show the 68% and 95% confidence intervals around it, respectively.

When allowing for more freedom in the equation of state, DESI BAO data alone cannot constrain the dark energy well, as there is an intrinsic degeneracy between the matter density, the dark energy evolution [e.g. 34, 94–97], and the absolute scaling set by the combination $H_0 r_d$ (shown in Fig. 2) [98, 99]. These degeneracies lead to very peculiar shapes of $f_{\text{DE}}(z)$ that can be compensated by anomalously large matter densities. Such dark energy models can fit the DESI data well, the best-fit having a $\Delta\chi^2 \simeq -5.5$ with respect to Λ CDM, while having 4 additional degrees of freedom.

However, when including distance measurements from SNe Ia these degeneracies are broken by a more accurate determination of $\Omega_{m,0}$ and $H_0 r_d$, and the dark energy evolution is much more tightly constrained, as shown in the middle column of Fig. 1. The best-fit model from the DESI+Union3 combination leads to an improvement in the fit of $\Delta\chi^2 \simeq -9.1$ with respect to Λ CDM. It is interesting to note that for both DESI BAO and DESI BAO+Union3,

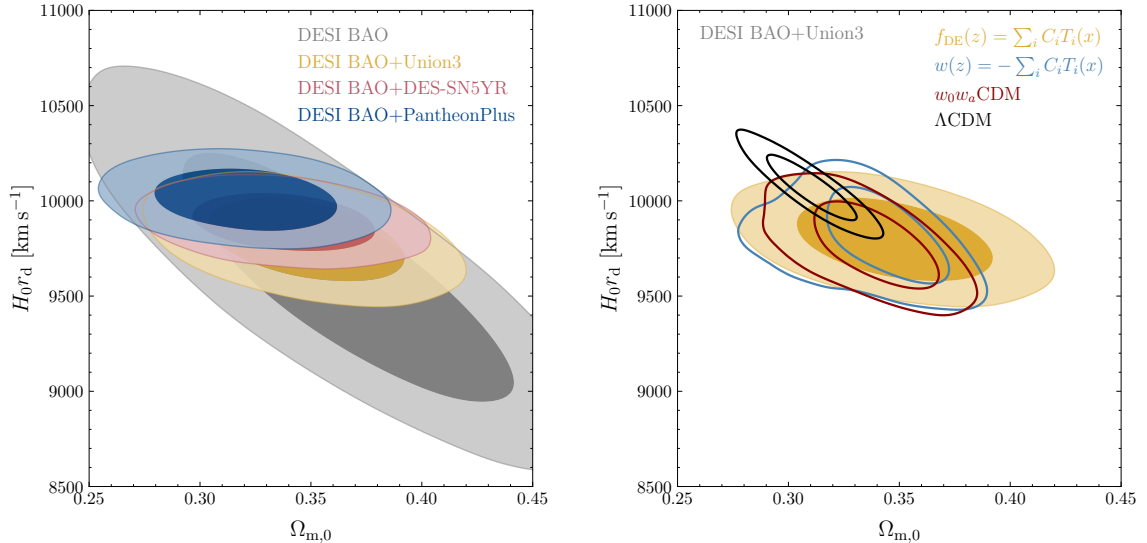


Figure 2. Marginalized posterior distributions for the cosmological parameters $H_0 r_d$ and $\Omega_{m,0}$ using a Chebyshev expansion of $f_{DE}(z)$ from the combination of DESI BAO and different supernova compilations (left). These constraints are independent of the early universe physics. In the right panel, we compare the constraints obtained from the Chebyshev expansion in $f_{DE}(z)$ and $w(z)$ to those obtained from restricting to Λ CDM (black) or $w_0 w_a$ CDM (red), using the DESI BAO+Union3 data combination.

a universe that returns to deceleration at present ($q_0 \geq 0$) is consistent with the data. At higher redshifts, the difference in $q(z \gtrsim 1)$ relative to Λ CDM reflects the preference for higher matter densities with respect to Λ CDM (also seen in $Om(z \gtrsim 1)$), which implies a longer epoch of matter domination ($q = 1/2$). In the rightmost panels, we show the reconstructions when including the measurements of the CMB anisotropies by Planck. These measurements probe physics at much higher redshifts ($z_{\text{rec}} \simeq 1100$), and provide a better estimation of the physical matter density $\omega_m = \Omega_{m,0} h^2$, as the height and position of the acoustic peaks are very sensitive to ω_{cdm} and ω_b . The spacing between these peaks is exquisitely measured by Planck [87], providing constraints on the late-time expansion history through the acoustic scale $\theta_s(z_{\text{rec}}) \propto 1/D_A(z_{\text{rec}})$, assuming standard pre-recombination physics. The CMB constraints, in combination with lower redshift SN and BAO measurements, lead to a much smoother reconstructed dark energy behaviour and a corresponding expansion history that mimics closely that of Λ CDM at higher redshifts. Our best-fit reconstruction leads to an improvement in the fit corresponding to a $\Delta\chi^2 \simeq -14.6$ compared to Λ CDM.

Table 2. Constraints on $\Omega_{m,0}$ and $H_0 r_d$ using the Chebyshev expansion up to four terms in the equation of state $w(z)$ and different non-CMB dataset combinations.

Data	$\Omega_{m,0}$	$H_0 r_d$ [km s^{-1}]
DESI BAO+Union3	$0.339^{+0.022}_{-0.015}$	9808 ± 150
DESI BAO+DES-SN5YR	$0.328^{+0.026}_{-0.011}$	9891 ± 100
DESI BAO+PantheonPlus	$0.327^{+0.017}_{-0.012}$	10030 ± 110

Moreover, combining BAO with SNe Ia measurements allows for a (relatively) model-

independent determination of $H_0 r_d$, with no assumptions on the physics of the early Universe and for an extended class of dark energy models. In [Table 2](#), we present the constraints on $H_0 r_d$ and $\Omega_{m,0}$ from various data combinations, also shown as 2D distributions in the right panel of [Fig. 2](#). Note that while our analysis was carried out using a much more flexible parametrization for the dark energy, the inferred values of $\Omega_{m,0}$ and $H_0 r_d$ are consistent with those reported in [\[78\]](#) in Λ CDM and $w_0 w_a$ CDM, as seen from the right panel of [Fig. 2](#).

Our methodology provides us with an extended class of expansion histories that are consistent with the data, and that lead to an improvement in fit. In [Table 3](#), we report the $\Delta\chi^2$ values for the different data combinations, relative to the best-fit χ^2 values in Λ CDM. Note that the results are quite consistent with the w_0-w_a approach, with crossing statistics having two more parameters than w_0-w_a but comparable χ^2 . Both approaches however have noticeably better fits than Λ CDM. Thus our reconstruction results with more freedom support the conclusions obtained using the standard w_0-w_a in [\[78\]](#). Furthermore, the more probes combined, the greater favouring of these models over Λ CDM. Irrespective of the dataset combination, the preference for a vanishing, or at least diminished, dark energy component in the past remains. Finally, let us note that due to the wide plotting range chosen for the equation of state ($-4 < w < 1$), the deviations from a cosmological constant, $w = -1$, may not look visually substantial. However, these deviations from Λ CDM are better reflected in the expansion history $h(z)$ and $Om(z)$ diagnostic (as seen from the third and fourth rows in [Fig. 1](#)).

Table 3. $\Delta\chi_{\text{MAP}}^2 \equiv \chi_{\text{model}}^2 - \chi_{\Lambda\text{CDM}}^2$ maximum a posteriori (MAP) values for the different models and data combinations. $\chi_{w(z)}^2$ refer to the runs using $w(z)$, while $\chi_{f_{\text{DE}}}^2$ refers to the modeling of $f_{\text{DE}}(z)$ using a Chebyshev expansion with four terms. The minimum χ^2 values were obtained using the minimizers [iminuit \[100\]](#) and [Py-BOBYQA \[101, 102\]](#). Note that all data combinations include DESI BAO measurements. (Recall $f_{\text{DE}}(z)$ analysis did not include CMB.)

Data	$\Delta\chi_{w(z)}^2$	$\Delta\chi_{f_{\text{DE}}}^2$	$\Delta\chi_{w_0 w_a}^2$	$\chi_{\Lambda\text{CDM}}^2$
DESI BAO	-5.5	-2.1	-3.7	12.7
+Union3	-9.1	-8.7	-9.0	41.0
+DES-SN5YR	-11.3	-10.8	-11.3	1659.7
+PantheonPlus	-5.4	-4.1	-3.6	1418.7
+Union3+Planck	-14.6	-	-15.7	2810.9
+DES-SN5YR+Planck	-17.9	-	-19.1	4430.7
+PantheonPlus+Planck	-11.1	-	-7.4	4188.4

3.2 Results using $f_{\text{DE}}(z)$

We now turn our attention to the dark energy density. We assess the robustness of our conclusions by allowing for the *effective* energy density to change sign and become negative. These behaviours are not possible to achieve by modeling the dark energy via its equation of state, as it inherently imposes $f_{\text{DE}} > 0$, as is evident from [Eq. \(2.4\)](#). In contrast with the previous section where we presented results with the Chebyshev expansion of $w(z)$, the direct reconstructions using Chebyshev expansion of $f_{\text{DE}}(z)$ are shown in [Fig. 3](#), where we plot the same quantities as in [Fig. 1](#), replacing $w(z)$ with $\Omega_{\text{DE}}(z)$ in the second row since the equation of state becomes singular when f_{DE} crosses zero. The overall conclusions drawn from the previous [Section 3.1](#) are unchanged. One notable difference is that the redshift

dependence of f_{DE} is much smoother. However, as discussed in Section 2.2.2, C_0 is no longer a free parameter but is derived by imposing $f_{\text{DE}}(z = 0) = 1$. Thus, strictly speaking, the modeling of f_{DE} has one less degree of freedom compared to that of $w(z)$. In the third column of Table 3, we report the $\Delta\chi^2$ values for the $f_{\text{DE}}(z)$ reconstructions, relative to the best-fit ΛCDM . Note that both the $w(z)$ and $f_{\text{DE}}(z)$ reconstructions lead to comparable χ^2 values for the combined BAO+SNe data, improving over ΛCDM .

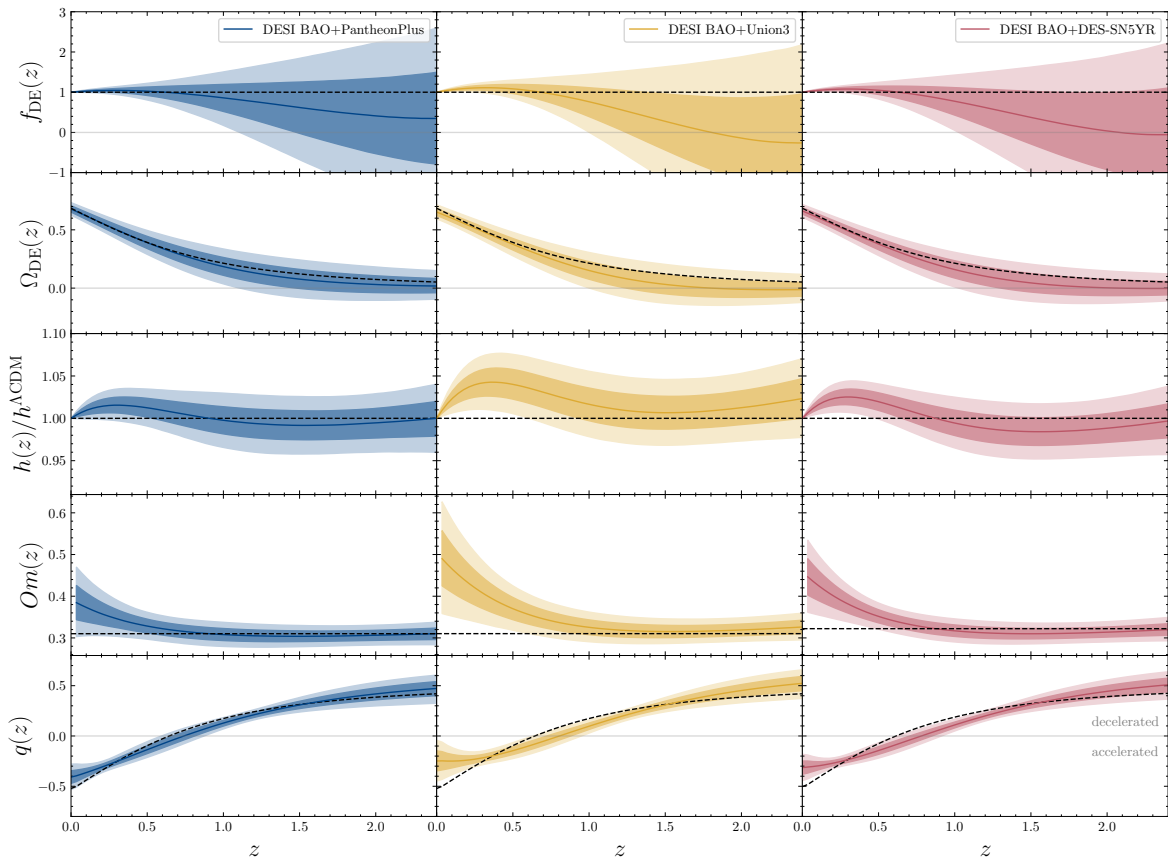


Figure 3. Dark energy reconstructions using the Chebyshev expansion of $f_{\text{DE}}(z)$ up to four terms with DESI BAO+Union3, DESI BAO+PantheonPlus and DESI BAO+DES-SN5YR datasets, respectively. The colored lines correspond to the median of the posterior distributions and the shaded regions show the 68% and 95% confidence intervals around it. The black-dashed lines depict the best-fit ΛCDM predictions for each data combination.

It is interesting to note that the data indeed allows the effective energy density to become negative at $z \gtrsim 1$, with the Union3 and DES-SN5YR compilations driving the preference for slightly more negative values with respect to PantheonPlus. Although our approach at this stage is purely phenomenological, negative energy densities can be achieved in various theoretically motivated scenarios, such as modified gravity [61–63], or by invoking the presence of a negative cosmological constant, with an additional degree of freedom driving the accelerated expansion at late-times [66, 103, 104]. As discussed in e.g. [105, 106], a change of sign in $\rho_{\text{DE}}^{\text{eff}}(z)$ could indicate non-trivial interactions in the dark sector.

While the reconstructions of $f_{\text{DE}}(z)$ seem consistent with a cosmological constant at higher redshifts, the reconstructed expansion history $h(z)$ at low redshift shows a $> 2\sigma$ deviation from the best-fit Λ CDM expansion history for each data combination, in part due to the different values of $\Omega_{\text{m},0}$. The deviations in $h(z)$ are more prominent since these not only reflect the deviations in $f_{\text{DE}}(z) \neq 1$, but also the deviations in $\Omega_{\text{m},0} \neq \Omega_{\text{m},0}^{\Lambda\text{CDM}}$. These deviations also (necessarily) translate into $\gtrsim 2\sigma$ deviations in the $Om(z \lesssim 0.5)$ diagnostic and deceleration parameter, $q(z \lesssim 0.3)$. Finally, in [Table 4](#) we report the marginalized constraints on the matter density $\Omega_{\text{m},0}$ and $H_0 r_{\text{d}}$ when allowing for negative energy densities. Note that DESI data alone does not have low redshift measurements and this allows flexible forms of expansion histories, such as those considered in this paper, to vary widely at very low redshifts, and this results in broad and weak constraints on $H_0 r_{\text{d}}$. Combined with supernova data, which has some measurements at low redshifts, tightens the constraints on $H_0 r_{\text{d}}$ as seen from [Fig. 2](#).

Table 4. Constraints on $\Omega_{\text{m},0}$ and $H_0 r_{\text{d}}$ using the Chebyshev expansion up to four terms in the dark energy density $f_{\text{DE}}(z)$, for different non-CMB dataset combinations.

Data	$\Omega_{\text{m},0}$	$H_0 r_{\text{d}}$ [km s^{-1}]
DESI BAO+Union3	0.347 ± 0.029	9795 ± 140
DESI BAO+DES-SN5YR	0.338 ± 0.027	9889 ± 100
DESI BAO+PantheonPlus	0.321 ± 0.027	10010 ± 110

4 Discussion and Conclusions

In this paper we use Crossing Statistics, implementing an expansion in terms of Chebyshev polynomials of the equation of state of dark energy $w(z)$, and dark energy density $f_{\text{DE}}(z)$, to reconstruct the expansion history of the universe and properties of dark energy using DESI BAO data combined with supernovae (Union3, PantheonPlus, or DES-SN5YR) and CMB Planck observations.

Our main result for dark energy is a clear and strong hint towards evolving dark energy, with rapidly falling energy density at $z \gtrsim 1$ (see [Fig. 1](#) middle panels). This behaviour can be modeled by a vanishing dark energy density (going to higher redshifts), with a phantom equation of state $w(z) < -1$ in the recent past. This preference is mainly driven by the non-CMB, “background-only” probes. Our results also suggest a hump in the expansion rate of the universe at $z \approx 0.2\text{--}0.3$ relative to the concordance model of cosmology. (This is not dependent on our specific choice of z_{max} , as shown in [Appendix B](#) with results little modified when using $z_{\text{max}} = 2.35$).

Including CMB observations does not alter this conclusion. However, the transition is smoother, and the expansion history is tightly constrained to mimic that of Λ CDM at high redshifts, albeit with different dark energy behaviour (see [Fig. 1](#) right panels). This is not unexpected since at high redshifts we do have a matter dominated universe and most models of dark energy (especially phantom ones) would not have much effect on the form of the expansion history. Our findings are consistent with and support the results reported in [\[78\]](#), showing a very good agreement with the analysis using the $w_0 w_a$ CDM parametrization.

When modeling the dark energy density $f_{\text{DE}}(z)$ as a Chebyshev series, and allowing $f_{\text{DE}}(z)$ to become negative in some redshift range, we find that the overall trend remains

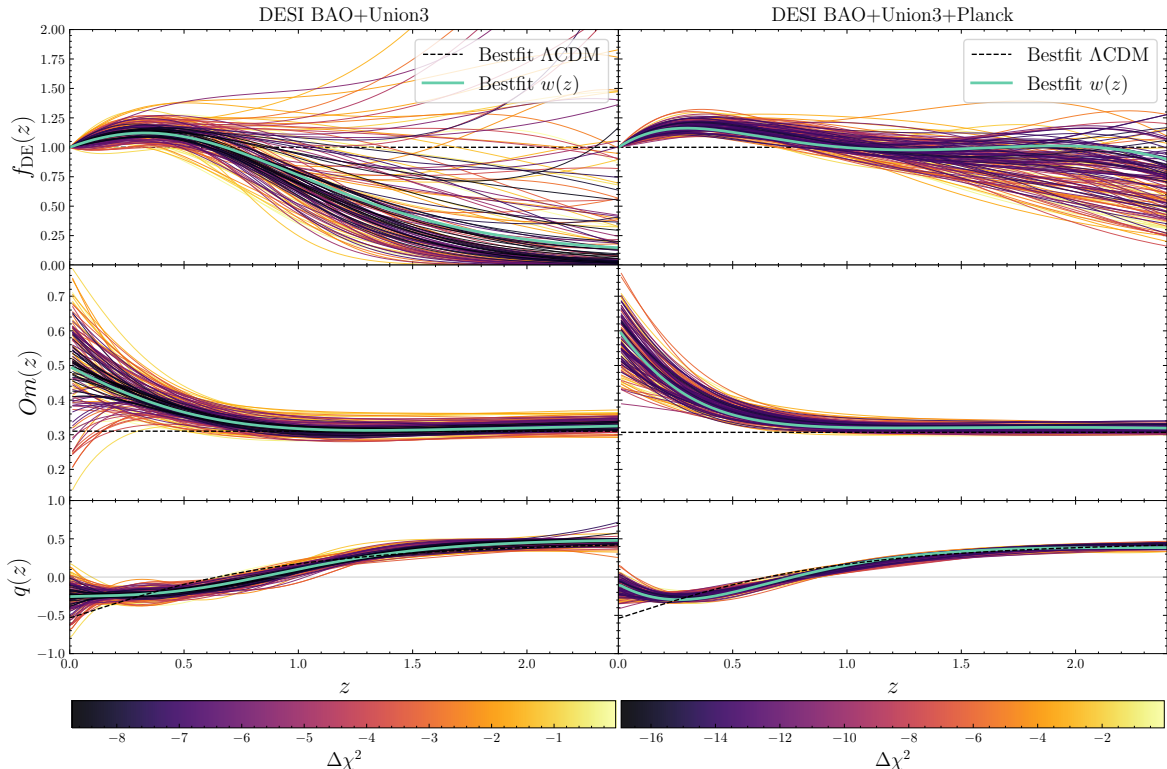


Figure 4. Instead of the marginalized error-bands, here we show some exact reconstructions of the expansion history, in terms of $f_{\text{DE}}(z)$, $Om(z)$, and $q(z)$, using the Chebyshev expansion of $w(z)$. Each reconstruction shown has a better likelihood than the best fit standard ΛCDM model (black dashed lines), color-coded in terms of $\Delta\chi^2$, with the green line showing the best fit from the chains.

the same, i.e. a vanishing dark energy density at $z \gtrsim 1.5$ (see Fig. 3). The behaviour of the expansion history from looking at Om diagnostic (being a function of the expansion history alone and sensitive to the combination of matter and dark energy densities) shows clear consistency with the ones obtained using a Chebyshev expansion of $w(z)$.

The non-CMB probes (SNe Ia and BAO) allow various shapes for the expansion history but also constrain in a model-independent manner the estimation of the absolute scaling set by the combination $H_0 r_d$, with no assumptions on the physics of the early universe (see Fig. 2). There is a noticeable shift in the $\Omega_{m,0} - H_0 r_d$ plane between our findings and estimation of these quantities when restricted to the ΛCDM model fitting Planck and ACT lensing data, quite possibly due in large part to a shift in $\Omega_{m,0}$.

Our results provide intriguing hints towards evolving dark energy; note that while they were obtained under the assumption of an especially flexible form for $w(z)$, this was still parametric and using any parametric form of $w(z)$ to study the unknown dark energy should be done cautiously. Follow-on work will explore this further. In this paper, we assumed a polynomial expansion (up to four terms, see Appendix A), which allows the equation of state to take on large negative values at high redshift and hence cause the dark energy density to approach zero.

While one would ideally like to choose maximally agnostic priors for the crossing hyperparameters, a significantly large part of the hyperparameter space may lead to similar physical quantities, due to the inherent nature of the equation of state (very negative equa-

tion of state gives very low energy density and hence little sensitivity). For example, $C_1 \gg 1$ or $C_3 \gg 1$ results in rapidly vanishing dark energy and similar predictions for the observables. As a result, such cases have very similar physical behaviour and would make posteriors unbounded. To prevent this from biasing our reconstructions, we imposed Gaussian priors on the Chebyshev coefficients centered around Λ CDM ($C_0 = 1, C_{i>0} = 0$). Such Gaussian priors effectively favour Λ CDM and ensure that any detected deviation from $w(z) = -1$ is mostly driven by the data. The marginalized posterior distributions for the Chebyshev coefficients are shown in [Appendix C](#).

To avoid loss of detail by only looking at the marginalized confidence levels, we can also look at the individual reconstructed expansion histories as presented in [Fig. 4](#). These lines are the exact expansion histories having a viable and acceptable fit to the combined data (in fact, with better χ^2 than Λ CDM). Having similar shapes and trends observed in [Fig. 4](#) and [Fig. 1](#) reflects that our choices of parametric form and priors have been reasonable for our case of study.

We emphasize that many of the aspects of intriguing dark energy behaviour seen here are also present in the standard w_0 - w_a analysis of [\[78\]](#), as shown in [Appendix E](#). For example, the rise toward $q(z=0) \approx 0$ corresponds to the leveling in $H(z)/(1+z)$ at low redshift and the less negative w_0 seen there. One can view this work as supporting the robustness of such indications in [\[78\]](#) even when more freedom is allowed in dark energy characteristics.

Our results also indicate that a broad range of expansion histories, substantially different from a cosmological constant, are viable and consistent with current data combinations. The trend of the reconstructed expansion history, $Om(z)$ diagnostic, and deceleration parameter $q(z)$ (see [Fig. 4](#) lower two panels), opens the door to models with a slowing down of cosmic acceleration [\[107\]](#). In fact, a universe with $q(z=0) > 0$ – after an accelerating period where $q(z) < 0$ – can be still consistent with the combined data. Such a temporary nature to cosmic acceleration could have some interesting theoretical implications worth exploring. At higher redshift, $z \gtrsim 1$, on the other hand, the trend of the reconstructed form of the dark energy density allows models with emergent dark energy behaviour [\[52, 53, 108, 109\]](#).

Further distance data, e.g. from DESI three-year measurements or the Nearby Supernova Factory [\[110\]](#), will allow deeper exploration into such model-independent expansion history reconstructions. Finally, let us note that the purpose of this work is not to perform model selection or to rule out Λ at high statistical significance, but to explore the allowed phenomenology of dark energy thoroughly, and compare to the standard w_0 - w_a parametrization. In a companion paper [\[111\]](#), we show that such phenomenology can be reproduced with merely one additional degree of freedom, with some physical motivation.

Acknowledgments

The authors would like to thank Benjamin L’Huillier for valuable discussions. We acknowledge the use of the Boltzmann solver `class` [\[57, 58\]](#) for the computation of theoretical observables, `cobaya` [\[89\]](#) for the sampling and `GetDist` [\[112\]](#) for the post-processing of our results. We also acknowledge the use of the standard `python` libraries for scientific computing, such as `numpy` [\[113\]](#), `scipy` [\[114\]](#) and `matplotlib` [\[115\]](#). This work was supported by the high-performance computing cluster Seondeok at the Korea Astronomy and Space Science Institute. A.S. would like to acknowledge the support by National Research Foundation of Korea 2021M3F7A1082056, and the support of the Korea Institute for Advanced Study

(KIAS) grant funded by the government of Korea.

This material is based upon work supported by the U.S. Department of Energy (DOE), Office of Science, Office of High-Energy Physics, under Contract No. DE-AC02-05CH11231, and by the National Energy Research Scientific Computing Center, a DOE Office of Science User Facility under the same contract. Additional support for DESI was provided by the U.S. National Science Foundation (NSF), Division of Astronomical Sciences under Contract No. AST-0950945 to the NSF’s National Optical-Infrared Astronomy Research Laboratory; the Science and Technology Facilities Council of the United Kingdom; the Gordon and Betty Moore Foundation; the Heising-Simons Foundation; the French Alternative Energies and Atomic Energy Commission (CEA); the National Council of Humanities, Science and Technology of Mexico (CONAHCYT); the Ministry of Science and Innovation of Spain (MICINN), and by the DESI Member Institutions: <https://www.desi.lbl.gov/collaborating-institutions>. Any opinions, findings, and conclusions or recommendations expressed in this material are those of the author(s) and do not necessarily reflect the views of the U. S. National Science Foundation, the U. S. Department of Energy, or any of the listed funding agencies.

The DESI collaboration is honored to be permitted to conduct scientific research on Iolkam Du’ag (Kitt Peak), a mountain with particular significance to the Tohono O’odham Nation.

Data Availability

The data used in this analysis will be made public along the Data Release 1 (details in <https://data.desi.lbl.gov/doc/releases/>).

A Order of the Chebyshev expansion

To justify our choice of truncating the Chebyshev series at four terms, in Fig. 5 we inspect the behaviour of the $\Delta\chi^2$ as a function of the number of free parameters for the DESI BAO+Union3 combination. While the expansion in $w(z)$ requires only 2 free parameters for the best-fit χ^2 to “converge” (as known from the success of w_0-w_a [see also 116]), the expansion of $f_{\text{DE}}(z)$ requires at least 3 free parameters to achieve similar performance. This also motivates why the $\Delta\chi^2$ ’s reported in Table 3 are similar for $w(z)$, $f_{\text{DE}}(z)$, and $w_0w_a\text{CDM}$.

Note that 3 free parameters in the expansion of $f_{\text{DE}}(z)$ correspond to the four C_i in Eq. (2.6) since C_0 is determined by Eq. (2.7). This is sufficient to ensure a similar performance between the $w(z)$ and $f_{\text{DE}}(z)$ modeling approaches, and a fair comparison of the different reconstructions. Thus, we restrict ourselves to a four-term Chebyshev expansion, after which the χ^2 does not change significantly by adding more degrees of freedom. This also matches previous findings in the context of CMB analyses [40].

B Robustness of z_{max}

To check that the results do not depend to any significant degree on the value of z_{max} , we show results in Fig. 6 that compare those using $z_{\text{max}} = 2.35$ to our standard $z_{\text{max}} = 3.5$. The general features of a strongly negative $w(z)$ at $z \gtrsim 0.7$, and hence vanishing dark energy density, and a rise in $w(z)$ at $z \lesssim 0.2$, are robust; these propagate to close similarity for

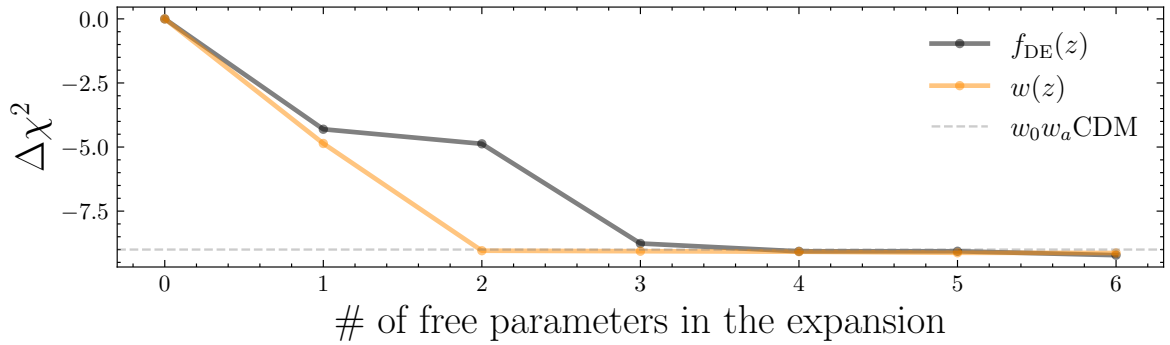


Figure 5. Change in the $\Delta\chi^2 \equiv \chi_{\text{cross}}^2 - \chi_{\Lambda\text{CDM}}^2$ value as a function of the number of free parameters introduced in the Chebyshev expansion, for the data combination DESI BAO+Union3.

$f_{\text{DE}}(z)$ and $h(z)$ as well. The conclusions on the matter density $\Omega_{\text{m},0}$ and $H_0 r_{\text{d}}$ also remain substantially unaffected, as seen in Fig. 7.

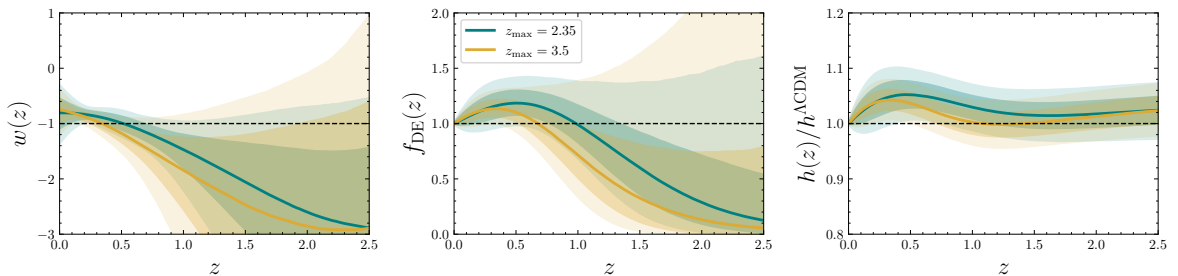


Figure 6. Effect of z_{max} on the dark energy reconstructions with the $w(z)$ crossing approach, shown for DESI BAO+Union3.

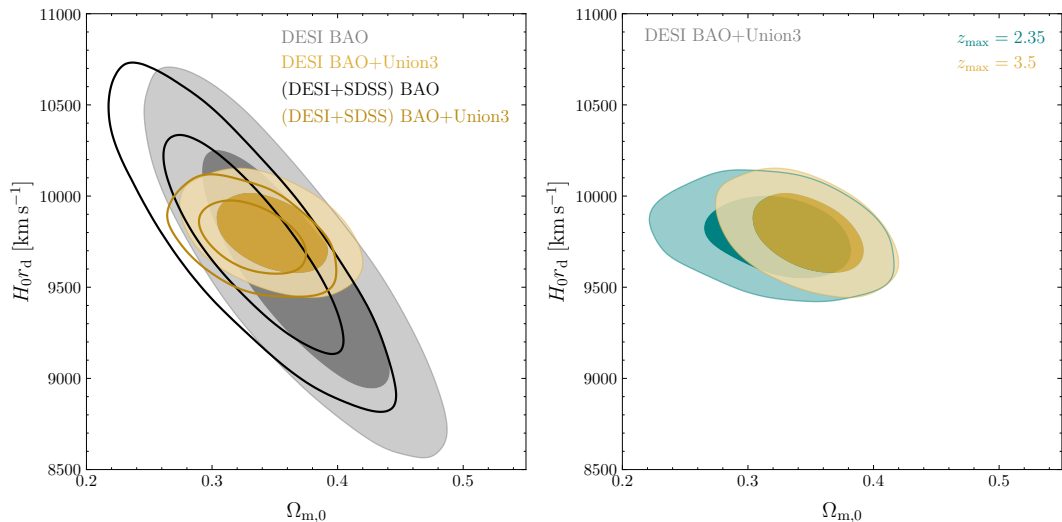


Figure 7. We compare the marginalized constraints on $H_0 r_{\text{d}}$ and $\Omega_{\text{m},0}$ when using DESI BAO vs (DESI+SDSS) BAO data (left panel) or the two different values of z_{max} (right panel), for the $f_{\text{DE}}(z)$ crossing approach.

C Crossing hyperparameters and effect of priors

We present the posterior distribution for Chebyshev polynomial coefficients for $w(z)$ (lower triangle) and $f_{\text{DE}}(z)$ (upper triangle) in Fig. 8 utilising the Gaussian priors from Table 1. Note that certain areas of the hyperparameter space produce comparable observables. This is especially evident in Eqs. (2.3) and (2.4) when C_i takes high values that cause $f_{\text{DE}}(z)$ to drop rapidly at higher redshift. Such vanishing dark energy yields indiscernible predictions for the observables ($D_{\text{M}}/r_{\text{d}}$, $D_{\text{H}}/r_{\text{d}}$, and $D_{\text{V}}/r_{\text{d}}$). This results in a large number of models with similar likelihood values and unbounded posterior distributions for the coefficients, unless the data has enough constraining power to break the $\Omega_{\text{m},0} - f_{\text{DE}}$ degeneracy. (The same effect is evident in [78] for w_0w_a CDM.) Thus, having a large number of hyperparameter combinations that result in similar observables can introduce unwanted biases in the marginalized posterior distributions of $w(z)/f_{\text{DE}}(z)$. To minimize potential prior-volume effects, we adopt Gaussian priors on the Chebyshev coefficients centered around the Λ CDM expected values $C_0 = 1$ and $C_{i>0} = 0$. This is, in fact, a conservative choice, as we are effectively penalizing large deviations from $C_0 = 1$ and $C_{i>0} = 0$, and intentionally favouring Λ CDM. Nonetheless, our choice of the Gaussian prior width is large enough that it allows us to cover a wide range of dark energy behaviours, as seen by the posterior distributions in Figs. 1 and 3. Our findings (see the $\Delta\chi^2$ in Table 3) indicate that despite having Gaussian priors on the C_i 's, the data still favours deviations from Λ CDM, adding to the robustness of our results.

D Comparison with (DESI+SDSS)

Figure 9 compares the results when using DESI BAO (as in the main text) vs the combination of (DESI+SDSS) BAO (as described in Section 2.3 and in detail in [78], this is not a mere addition of the two sets but a combination of the most impactful points from both sets). The results are quite consistent, in particular when considering the full DESI BAO+Union3+Planck data combination. The conclusions on the matter density $\Omega_{\text{m},0}$ and H_0r_{d} also remain substantially unaffected, as was seen in Fig. 7. We refer the reader to Appendix A in [78] for a more thorough comparison of the (DESI+SDSS) vs DESI BAO results.

E Comparison with w_0w_a CDM

In Figure 10, we show how our results compare to the results using the conventional w_0w_a CDM parametrization.

References

- [1] SUPERNOVA SEARCH TEAM collaboration, *Observational evidence from supernovae for an accelerating universe and a cosmological constant*, *Astron. J.* **116** (1998) 1009 [[astro-ph/9805201](#)].
- [2] SUPERNOVA COSMOLOGY PROJECT collaboration, *Measurements of Ω and Λ from 42 High Redshift Supernovae*, *Astrophys. J.* **517** (1999) 565 [[astro-ph/9812133](#)].
- [3] N. Aghanim, Y. Akrami, F. Arroja, M. Ashdown, J. Aumont, C. Baccigalupi et al., *Planck2018 results: I. overview and the cosmological legacy of planck*, *Astronomy & Astrophysics* **641** (2020) A1.

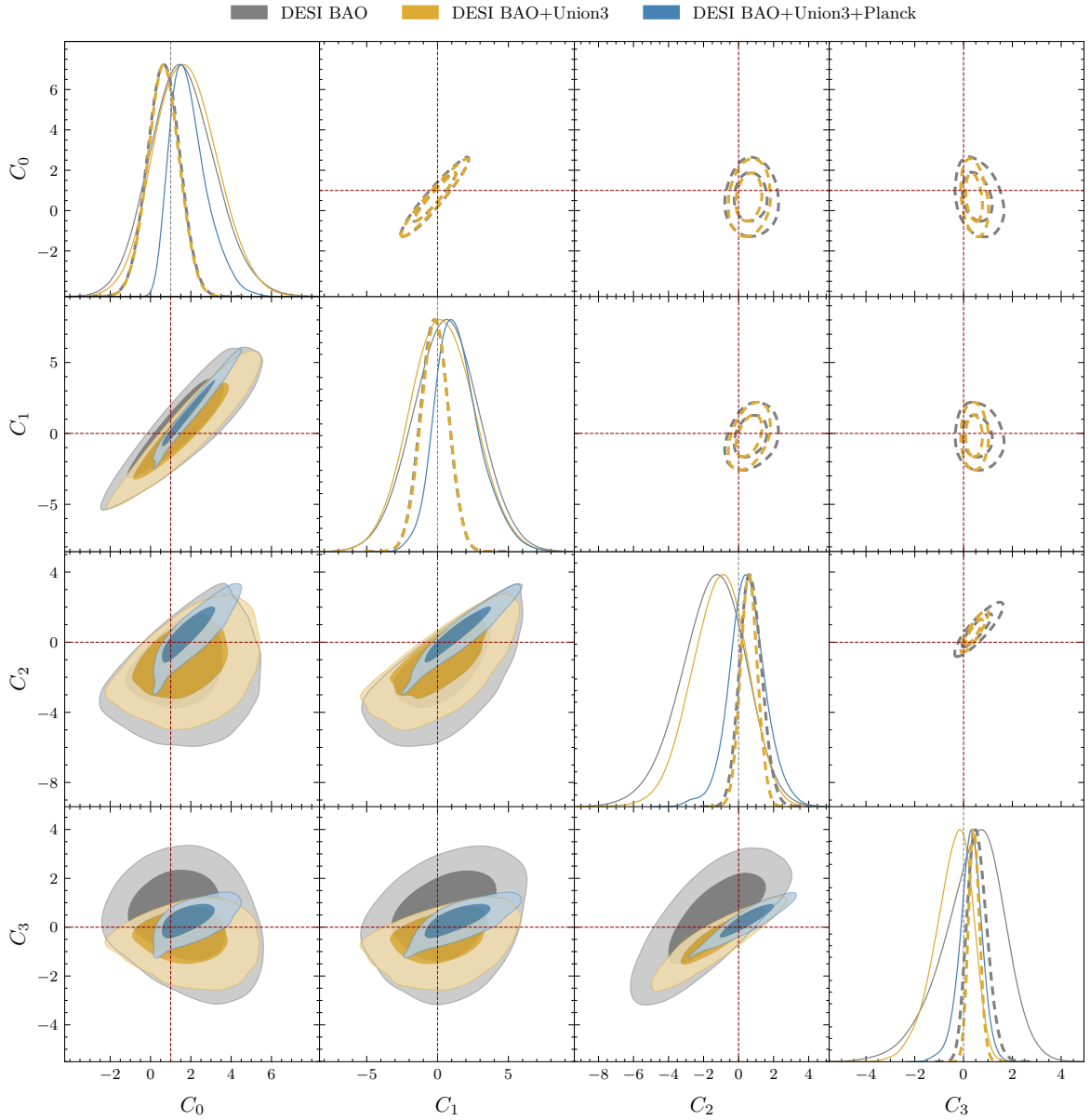


Figure 8. Marginalized posterior distributions on the Chebyshev coefficients for the $w(z)$ (solid contours, lower triangle) and the $f_{\text{DE}}(z)$ (dashed contours, upper triangle) Chebyshev expansions. The red-dashed lines give the values taken by the mean function (Λ CDM).

- [4] S. Alam, M. Aubert, S. Avila, C. Balland, J.E. Bautista, M.A. Bershadsky et al., *Completed sdss-iv extended baryon oscillation spectroscopic survey: Cosmological implications from two decades of spectroscopic surveys at the apache point observatory*, *Physical Review D* **103** (2021) .
- [5] C. Zhao, A. Variu, M. He, D. Forero-Sánchez, A. Tamone, C.-H. Chuang et al., *The completed sdss-iv extended baryon oscillation spectroscopic survey: cosmological implications from multitracers baryon oscillation analysis with galaxies and voids*, *Monthly Notices of the Royal Astronomical Society* **511** (2022) 5492–5524.

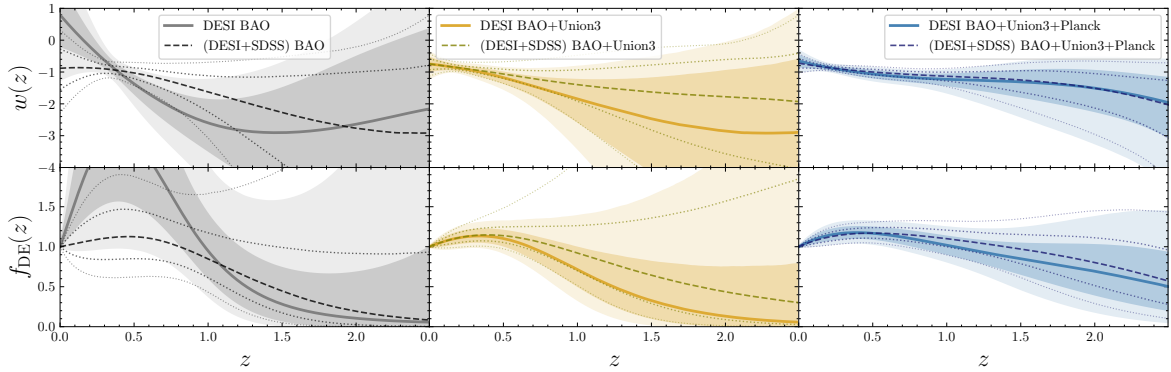


Figure 9. Comparison of the dark energy reconstructions using the Chebyshev expansion of $w(z)$ from (DESI+SDSS) BAO (dashed lines) vs DESI BAO (solid-filled contours).

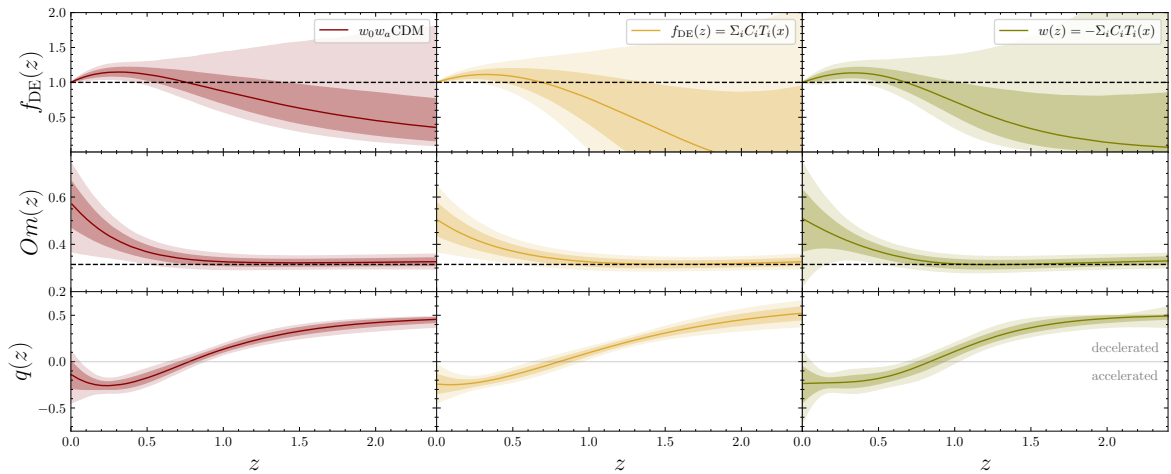


Figure 10. Comparison of the dark energy reconstructions using the conventional w_0-w_a parametrization, a Chebyshev expansion of $f_{\text{DE}}(z)$ and a Chebyshev expansion of $w(z)$ from using DESI BAO+Union3 data.

- [6] J.P. Ostriker and P.J. Steinhardt, *The Observational case for a low density universe with a nonzero cosmological constant*, *Nature* **377** (1995) 600.
- [7] S. Weinberg, *The cosmological constant problem*, *Rev. Mod. Phys.* **61** (1989) 1.
- [8] V. Sahni and A.A. Starobinsky, *The Case for a positive cosmological Lambda term*, *Int. J. Mod. Phys. D* **9** (2000) 373 [[astro-ph/9904398](#)].
- [9] P.J.E. Peebles and B. Ratra, *The Cosmological Constant and Dark Energy*, *Rev. Mod. Phys.* **75** (2003) 559 [[astro-ph/0207347](#)].
- [10] E.J. Copeland, M. Sami and S. Tsujikawa, *Dynamics of dark energy*, *Int. J. Mod. Phys. D* **15** (2006) 1753 [[hep-th/0603057](#)].
- [11] P. Bull et al., *Beyond Λ CDM: Problems, solutions, and the road ahead*, *Phys. Dark Univ.* **12** (2016) 56 [[1512.05356](#)].
- [12] L. Perivolaropoulos and F. Skara, *Challenges for Λ CDM: An update*, *New Astron. Rev.* **95** (2022) 101659 [[2105.05208](#)].

- [13] DES collaboration, *Dark Energy Survey year 1 results: Cosmological constraints from galaxy clustering and weak lensing*, *Phys. Rev. D* **98** (2018) 043526 [[1708.01530](#)].
- [14] DES collaboration, *Dark Energy Survey Year 1 results: Cosmological constraints from cosmic shear*, *Phys. Rev. D* **98** (2018) 043528 [[1708.01538](#)].
- [15] EBOSS collaboration, *Completed SDSS-IV extended Baryon Oscillation Spectroscopic Survey: Cosmological implications from two decades of spectroscopic surveys at the Apache Point Observatory*, *Phys. Rev. D* **103** (2021) 083533 [[2007.08991](#)].
- [16] C. Heymans et al., *KiDS-1000 Cosmology: Multi-probe weak gravitational lensing and spectroscopic galaxy clustering constraints*, *Astron. Astrophys.* **646** (2021) A140 [[2007.15632](#)].
- [17] DES collaboration, *Dark Energy Survey Year 3 results: Cosmological constraints from galaxy clustering and weak lensing*, *Phys. Rev. D* **105** (2022) 023520 [[2105.13549](#)].
- [18] DESI Collaboration, *DESI 2024 I: Data Release 1 of the Dark Energy Spectroscopic Instrument, in preparation* (2025) .
- [19] D. Huterer and G. Starkman, *Parameterization of dark-energy properties: A Principal-component approach*, *Phys. Rev. Lett.* **90** (2003) 031301 [[astro-ph/0207517](#)].
- [20] A. Shafieloo, U. Alam, V. Sahni and A.A. Starobinsky, *Smoothing Supernova Data to Reconstruct the Expansion History of the Universe and its Age*, *Mon. Not. Roy. Astron. Soc.* **366** (2006) 1081 [[astro-ph/0505329](#)].
- [21] A. Shafieloo, *Model-independent reconstruction of the expansion history of the Universe and the properties of dark energy*, *MNRAS* **380** (2007) 1573 [[astro-ph/0703034](#)].
- [22] R.G. Crittenden, L. Pogosian and G.-B. Zhao, *Investigating dark energy experiments with principal components*, *J. Cosmology Astropart. Phys.* **2009** (2009) 025 [[astro-ph/0510293](#)].
- [23] C. Bogdanos and S. Nesseris, *Genetic Algorithms and Supernovae Type Ia Analysis*, *JCAP* **05** (2009) 006 [[0903.2805](#)].
- [24] T. Holsclaw, U. Alam, B. Sansó, H. Lee, K. Heitmann, S. Habib et al., *Nonparametric reconstruction of the dark energy equation of state*, *Phys. Rev. D* **82** (2010) 103502 [[1009.5443](#)].
- [25] T. Holsclaw, U. Alam, B. Sansó, H. Lee, K. Heitmann, S. Habib et al., *Nonparametric dark energy reconstruction from supernova data*, *Phys. Rev. Lett.* **105** (2010) 241302.
- [26] S. Nesseris and A. Shafieloo, *A model independent null test on the cosmological constant*, *Mon. Not. Roy. Astron. Soc.* **408** (2010) 1879 [[1004.0960](#)].
- [27] A. Shafieloo, A.G. Kim and E.V. Linder, *Gaussian Process Cosmography*, *Phys. Rev. D* **85** (2012) 123530 [[1204.2272](#)].
- [28] G.-B. Zhao, R.G. Crittenden, L. Pogosian and X. Zhang, *Examining the Evidence for Dynamical Dark Energy*, *Phys. Rev. Lett.* **109** (2012) 171301 [[1207.3804](#)].
- [29] G.-B. Zhao, R.G. Crittenden, L. Pogosian and X. Zhang, *Examining the evidence for dynamical dark energy*, *Phys. Rev. Lett.* **109** (2012) 171301 [[1207.3804](#)].
- [30] S. Nesseris and J. García-Bellido, *A new perspective on dark energy modeling via genetic algorithms*, *Journal of Cosmology and Astroparticle Physics* **2012** (2012) 033–033.
- [31] A. Shafieloo, A.G. Kim and E.V. Linder, *Model independent tests of cosmic growth versus expansion*, *Phys. Rev. D* **87** (2013) 023520 [[1211.6128](#)].
- [32] B. L’Huillier and A. Shafieloo, *Model-independent test of the FLRW metric, the flatness of the Universe, and non-local measurement of H_{0r_d}* , *JCAP* **01** (2017) 015 [[1606.06832](#)].
- [33] H. Koo, A. Shafieloo, R.E. Keeley and B. L’Huillier, *Model selection and parameter estimation using the iterative smoothing method*, *JCAP* **03** (2021) 034 [[2009.12045](#)].

- [34] R. Calderón, B. L’Huillier, D. Polarski, A. Shafieloo and A.A. Starobinsky, *Joint reconstructions of growth and expansion histories from stage-IV surveys with minimal assumptions: Dark energy beyond Λ* , *Phys. Rev. D* **106** (2022) 083513 [[2206.13820](#)].
- [35] R. Calderón, B. L’Huillier, D. Polarski, A. Shafieloo and A.A. Starobinsky, *Joint reconstructions of growth and expansion histories from stage-IV surveys with minimal assumptions. II. Modified gravity and massive neutrinos*, *Phys. Rev. D* **108** (2023) 023504 [[2301.00640](#)].
- [36] A. Shafieloo, *Crossing Statistic: Bayesian interpretation, model selection and resolving dark energy parametrization problem*, *J. Cosmology Astropart. Phys.* **05** (2012) 024 [[1202.4808](#)].
- [37] A. Shafieloo, *Crossing statistic: reconstructing the expansion history of the universe*, *J. Cosmology Astropart. Phys.* **2012** (2012) 002 [[1204.1109](#)].
- [38] A. Shafieloo, T. Clifton and P.G. Ferreira, *The Crossing Statistic: Dealing with Unknown Errors in the Dispersion of Type Ia Supernovae*, *J. Cosmology Astropart. Phys.* **08** (2011) 017 [[1006.2141](#)].
- [39] D.K. Hazra and A. Shafieloo, *Test of consistency between Planck and WMAP*, *Phys. Rev. D* **89** (2014) 043004 [[1308.2911](#)].
- [40] D.K. Hazra and A. Shafieloo, *Confronting the concordance model of cosmology with Planck data*, *JCAP* **01** (2014) 043 [[1401.0595](#)].
- [41] A. Shafieloo and D.K. Hazra, *Consistency of the Planck CMB data and Λ CDM cosmology*, *JCAP* **04** (2017) 012 [[1610.07402](#)].
- [42] S. Haude, S. Salehi, S. Vidal, M. Maturi and M. Bartelmann, *Model-Independent Determination of the Cosmic Growth Factor*, [1912.04560](#).
- [43] LSST Science Collaboration, *LSST Science Book, Version 2.0*, *arXiv e-prints* (2009) [arXiv:0912.0201](#) [[0912.0201](#)].
- [44] EUCLID collaboration, *Euclid preparation. I. The Euclid Wide Survey*, *Astron. Astrophys.* **662** (2022) A112 [[2108.01201](#)].
- [45] J. Lazio, *The Square Kilometre Array*, in *Panoramic Radio Astronomy: Wide-field 1-2 GHz Research on Galaxy Evolution*, p. 58, Jan., 2009, DOI [[0910.0632](#)].
- [46] Y. Wang et al., *The High Latitude Spectroscopic Survey on the Nancy Grace Roman Space Telescope*, *Astrophys. J.* **928** (2022) 1 [[2110.01829](#)].
- [47] M. Chevallier and D. Polarski, *Accelerating Universes with Scaling Dark Matter*, *International Journal of Modern Physics D* **10** (2001) 213 [[gr-qc/0009008](#)].
- [48] E.V. Linder, *Exploring the expansion history of the universe*, *Phys. Rev. Lett.* **90** (2003) 091301 [[astro-ph/0208512](#)].
- [49] R. de Putter and E.V. Linder, *Calibrating Dark Energy*, *JCAP* **10** (2008) 042 [[0808.0189](#)].
- [50] A. Shafieloo, *Model Independent Reconstruction of the Expansion History of the Universe and the Properties of Dark Energy*, *Mon. Not. Roy. Astron. Soc.* **380** (2007) 1573 [[astro-ph/0703034](#)].
- [51] G.-B. Zhao et al., *Dynamical dark energy in light of the latest observations*, *Nature Astron.* **1** (2017) 627 [[1701.08165](#)].
- [52] V. Poulin, K.K. Boddy, S. Bird and M. Kamionkowski, *Implications of an extended dark energy cosmology with massive neutrinos for cosmological tensions*, *Phys. Rev. D* **97** (2018) 123504 [[1803.02474](#)].
- [53] Y. Wang, L. Pogosian, G.-B. Zhao and A. Zucca, *Evolution of dark energy reconstructed from the latest observations*, *Astrophys. J. Lett.* **869** (2018) L8 [[1807.03772](#)].

- [54] R.E. Keeley, S. Joudaki, M. Kaplinghat and D. Kirkby, *Implications of a transition in the dark energy equation of state for the H_0 and σ_8 tensions*, *JCAP* **12** (2019) 035 [[1905.10198](#)].
- [55] B. L’Huillier, A. Shafieloo, D. Polarski and A.A. Starobinsky, *Defying the laws of Gravity I: Model-independent reconstruction of the Universe expansion from growth data*, *Mon. Not. Roy. Astron. Soc.* **494** (2020) 819 [[1906.05991](#)].
- [56] M. Raveri, L. Pogosian, M. Martinelli, K. Koyama, A. Silvestri and G.-B. Zhao, *Principal reconstructed modes of dark energy and gravity*, *Journal of Cosmology and Astroparticle Physics* **2023** (2023) 061.
- [57] J. Lesgourgues, *The Cosmic Linear Anisotropy Solving System (CLASS) I: Overview*, *arXiv e-prints* (2011) arXiv:1104.2932 [[1104.2932](#)].
- [58] D. Blas, J. Lesgourgues and T. Tram, *The Cosmic Linear Anisotropy Solving System (CLASS). Part II: Approximation schemes*, *J. Cosmology Astropart. Phys.* **2011** (2011) 034 [[1104.2933](#)].
- [59] R.E. Keeley and A. Shafieloo, *Ruling Out New Physics at Low Redshift as a Solution to the H_0 Tension*, *Phys. Rev. Lett.* **131** (2023) 111002 [[2206.08440](#)].
- [60] W. Hu and I. Sawicki, *A Parameterized Post-Friedmann Framework for Modified Gravity*, *Phys. Rev. D* **76** (2007) 104043 [[0708.1190](#)].
- [61] V. Sahni and Y. Shtanov, *Braneworld models of dark energy*, *Journal of Cosmology and Astroparticle Physics* **2003** (2003) 014.
- [62] S.-Y. Zhou, E.J. Copeland and P.M. Saffin, *Cosmological constraints on $f(G)$ dark energy models*, *Journal of Cosmology and Astroparticle Physics* **2009** (2009) 009.
- [63] F. Bauer, J. Solà and H. Štefancić, *Dynamically avoiding fine-tuning the cosmological constant: the ‘‘relaxed universe’’*, *Journal of Cosmology and Astroparticle Physics* **2010** (2010) 029.
- [64] J. Matsumoto, *Phantom crossing dark energy in horndeski’s theory*, *Physical Review D* **97** (2018) .
- [65] Y. Tiwari, B. Ghosh and R.K. Jain, *Towards a possible solution to the hubble tension with horndeski gravity*, *The European Physical Journal C* **84** (2024) .
- [66] R. Calderón, R. Gannouji, B. L’Huillier and D. Polarski, *Negative cosmological constant in the dark sector?*, *Phys. Rev. D* **103** (2021) 023526 [[2008.10237](#)].
- [67] J.A. Vazquez, S. Hee, M.P. Hobson, A.N. Lasenby, M. Ibison and M. Bridges, *Observational constraints on conformal time symmetry, missing matter and double dark energy*, *JCAP* **07** (2018) 062 [[1208.2542](#)].
- [68] V. Sahni, A. Shafieloo and A.A. Starobinsky, *Model independent evidence for dark energy evolution from Baryon Acoustic Oscillations*, *Astrophys. J. Lett.* **793** (2014) L40 [[1406.2209](#)].
- [69] J. Sola, A. Gomez-Valent and J. de Cruz Pérez, *Hints of dynamical vacuum energy in the expanding Universe*, *Astrophys. J. Lett.* **811** (2015) L14 [[1506.05793](#)].
- [70] A. Lymperis, *Late-time cosmology with phantom dark-energy in $f(q)$ gravity*, *Journal of Cosmology and Astroparticle Physics* **2022** (2022) 018.
- [71] O. Akarsu, T. Dereli and J.A. Vazquez, *A divergence-free parametrization for dynamical dark energy*, *Journal of Cosmology and Astroparticle Physics* **2015** (2015) 049–049.
- [72] K.J. Ludwick, *The viability of phantom dark energy: A review*, *Modern Physics Letters A* **32** (2017) 1730025.
- [73] A. Gomez-Valent and J. Sola Peracaula, *Phantom matter: a challenging solution to the cosmological tensions*, [2404.18845](#).

- [74] DESI Collaboration, A. Aghamousa, J. Aguilar, S. Ahlen, S. Alam, L.E. Allen et al., *The DESI Experiment Part I: Science, Targeting, and Survey Design*, *arXiv e-prints* (2016) arXiv:1611.00036 [[1611.00036](#)].
- [75] DESI Collaboration, B. Abareshi, J. Aguilar, S. Ahlen, S. Alam, D.M. Alexander et al., *Overview of the Instrumentation for the Dark Energy Spectroscopic Instrument*, *AJ* **164** (2022) 207 [[2205.10939](#)].
- [76] DESI Collaboration, A.G. Adame, J. Aguilar, S. Ahlen, S. Alam, G. Aldering et al., *Validation of the Scientific Program for the Dark Energy Spectroscopic Instrument*, *AJ* **167** (2024) 62 [[2306.06307](#)].
- [77] DESI Collaboration, A.G. Adame, J. Aguilar, S. Ahlen, S. Alam, G. Aldering et al., *The Early Data Release of the Dark Energy Spectroscopic Instrument*, *arXiv e-prints* (2023) arXiv:2306.06308 [[2306.06308](#)].
- [78] DESI Collaboration, A.G. Adame, J. Aguilar, S. Ahlen, S. Alam, D.M. Alexander et al., *DESI 2024 VI: Cosmological Constraints from the Measurements of Baryon Acoustic Oscillations*, *arXiv e-prints* (2024) arXiv:2404.03002 [[2404.03002](#)].
- [79] DESI Collaboration, A.G. Adame, J. Aguilar, S. Ahlen, S. Alam, D.M. Alexander et al., *DESI 2024 III: Baryon Acoustic Oscillations from Galaxies and Quasars*, *arXiv e-prints* (2024) arXiv:2404.03000 [[2404.03000](#)].
- [80] DESI Collaboration, A.G. Adame, J. Aguilar, S. Ahlen, S. Alam, D.M. Alexander et al., *DESI 2024 IV: Baryon Acoustic Oscillations from the Lyman Alpha Forest*, *arXiv e-prints* (2024) arXiv:2404.03001 [[2404.03001](#)].
- [81] DESI Collaboration, *DESI 2024 II: Sample definitions, characteristics and two-point clustering statistics, in preparation* (2024) .
- [82] DESI Collaboration, *DESI 2024 V: Analysis of the full shape of two-point clustering statistics from galaxies and quasars, in preparation* (2024) .
- [83] DESI Collaboration, *DESI 2024 VII: Cosmological constraints from full-shape analyses of the two-point clustering statistics measurements, in preparation* (2024) .
- [84] D. Brout et al., *The Pantheon+ Analysis: Cosmological Constraints*, *Astrophys. J.* **938** (2022) 110 [[2202.04077](#)].
- [85] D. Rubin et al., *Union Through UNITY: Cosmology with 2,000 SNe Using a Unified Bayesian Framework*, [2311.12098](#).
- [86] DES collaboration, *The Dark Energy Survey: Cosmology Results With ~1500 New High-redshift Type Ia Supernovae Using The Full 5-year Dataset*, [2401.02929](#).
- [87] PLANCK collaboration, *Planck 2018 results. VI. Cosmological parameters*, *Astron. Astrophys.* **641** (2020) A6 [[1807.06209](#)].
- [88] PLANCK collaboration, *Planck 2018 results. V. CMB power spectra and likelihoods*, *Astron. Astrophys.* **641** (2020) A5 [[1907.12875](#)].
- [89] J. Torrado and A. Lewis, *Cobaya: Code for Bayesian Analysis of hierarchical physical models*, *J. Cosmology Astropart. Phys.* **05** (2021) 057 [[2005.05290](#)].
- [90] A. Lewis and S. Bridle, *Cosmological parameters from CMB and other data: A Monte Carlo approach*, *Phys. Rev.* **D66** (2002) 103511 [[astro-ph/0205436](#)].
- [91] A. Lewis, *Efficient sampling of fast and slow cosmological parameters*, *Phys. Rev.* **D87** (2013) 103529 [[1304.4473](#)].
- [92] R.M. Neal, *Taking Bigger Metropolis Steps by Dragging Fast Variables*, *ArXiv Mathematics e-prints* (2005) [[math/0502099](#)].

- [93] V. Sahni, A. Shafieloo and A.A. Starobinsky, *Two new diagnostics of dark energy*, *Phys. Rev. D* **78** (2008) 103502 [[0807.3548](#)].
- [94] I. Wasserman, *On the degeneracy inherent in observational determination of the dark energy equation of state*, *Phys. Rev. D* **66** (2002) 123511 [[astro-ph/0203137](#)].
- [95] M. Kunz, *Degeneracy between the dark components resulting from the fact that gravity only measures the total energy-momentum tensor*, *Phys. Rev. D* **80** (2009) 123001.
- [96] A. Shafieloo and E.V. Linder, *Cosmographic Degeneracy*, *Phys. Rev. D* **84** (2011) 063519 [[1107.1033](#)].
- [97] R. von Marttens, L. Lombriser, M. Kunz, V. Marra, L. Casarini and J. Alcaniz, *Dark degeneracy i: Dynamical or interacting dark energy?*, *Physics of the Dark Universe* **28** (2020) 100490.
- [98] W.J. Percival, R.C. Nichol, D.J. Eisenstein, D.H. Weinberg, M. Fukugita, A.C. Pope et al., *Measuring the matter density using baryon oscillations in the sdss*, *The Astrophysical Journal* **657** (2007) 51–55.
- [99] A. Cuceu, J. Farr, P. Lemos and A. Font-Ribera, *Baryon acoustic oscillations and the hubble constant: past, present and future*, *Journal of Cosmology and Astroparticle Physics* **2019** (2019) 044–044.
- [100] H. Dembinski and P.O. et al., *scikit-hep/iminuit*, .
- [101] C. Cartis, J. Fiala, B. Marteau and L. Roberts, *Improving the flexibility and robustness of model-based derivative-free optimization solvers*, 2018.
- [102] C. Cartis, L. Roberts and O. Sheridan-Methven, *Escaping local minima with local derivative-free methods: a numerical investigation*, *Optimization* **71** (2021) 2343–2373.
- [103] J. Grande, J. Sola and H. Stefancic, *LXCDM: A Cosmon model solution to the cosmological coincidence problem?*, *JCAP* **08** (2006) 011 [[gr-qc/0604057](#)].
- [104] L. Visinelli, S. Vagnozzi and U. Danielsson, *Revisiting a negative cosmological constant from low-redshift data*, *Symmetry* **11** (2019) 1035 [[1907.07953](#)].
- [105] S.M. Carroll, A. De Felice, V. Duvvuri, D.A. Easson, M. Trodden and M.S. Turner, *The Cosmology of generalized modified gravity models*, *Phys. Rev. D* **71** (2005) 063513 [[astro-ph/0410031](#)].
- [106] S. Das, P.S. Corasaniti and J. Khoury, *Superacceleration as the signature of a dark sector interaction*, *Phys. Rev. D* **73** (2006) 083509.
- [107] A. Shafieloo, V. Sahni and A.A. Starobinsky, *Is cosmic acceleration slowing down?*, *Phys. Rev. D* **80** (2009) 101301 [[0903.5141](#)].
- [108] X. Li and A. Shafieloo, *A Simple Phenomenological Emergent Dark Energy Model can Resolve the Hubble Tension*, *Astrophys. J. Lett.* **883** (2019) L3 [[1906.08275](#)].
- [109] X. Li and A. Shafieloo, *Evidence for Emergent Dark Energy*, *Astrophys. J.* **902** (2020) 58 [[2001.05103](#)].
- [110] NEARBY SUPERNOVA FACTORY collaboration, *Uniform Recalibration of Common Spectrophotometry Standard Stars onto the CALSPEC System Using the SuperNova Integral Field Spectrograph*, *Astrophys. J. Supp.* **263** (2022) 1 [[2205.01116](#)].
- [111] K. Lodha, A. Shafieloo, R. Calderon, E. Linder, W. Sohn, J.L. Cervantes-Cota et al., *DESI 2024: Constraints on Physics-Focused Aspects of Dark Energy using DESI DR1 BAO Data*, *arXiv e-prints* (2024) arXiv:2405.13588 [[2405.13588](#)].
- [112] A. Lewis, *GetDist: a Python package for analysing Monte Carlo samples*, 2019.

- [113] C.R. Harris, K.J. Millman, S.J. van der Walt, R. Gommers, P. Virtanen, D. Cournapeau et al., *Array programming with NumPy*, *Nature* **585** (2020) 357.
- [114] P. Virtanen, R. Gommers, T.E. Oliphant, M. Haberland, T. Reddy, D. Cournapeau et al., *SciPy 1.0: Fundamental Algorithms for Scientific Computing in Python*, *Nature Methods* **17** (2020) 261.
- [115] J.D. Hunter, *Matplotlib: A 2d graphics environment*, *Computing in Science & Engineering* **9** (2007) 90.
- [116] E.V. Linder and D. Huterer, *How many dark energy parameters?*, *Phys. Rev. D* **72** (2005) 043509 [[astro-ph/0505330](#)].

F Author Affiliations

- ¹Korea Astronomy and Space Science Institute, 776, Daedeokdae-ro, Yuseong-gu, Daejeon 34055, Republic of Korea
- ²University of Science and Technology, 217 Gajeong-ro, Yuseong-gu, Daejeon 34113, Republic of Korea
- ³Lawrence Berkeley National Laboratory, 1 Cyclotron Road, Berkeley, CA 94720, USA
- ⁴Space Sciences Laboratory, University of California, Berkeley, 7 Gauss Way, Berkeley, CA 94720, USA
- ⁵University of California, Berkeley, 110 Sproul Hall #5800 Berkeley, CA 94720, USA
- ⁶IRFU, CEA, Université Paris-Saclay, F-91191 Gif-sur-Yvette, France
- ⁷Departamento de Física, Instituto Nacional de Investigaciones Nucleares, Carretera México-Toluca S/N, La Marquesa, Ocoyoacac, Edo. de México C.P. 52750, México
- ⁸Institute of Cosmology and Gravitation, University of Portsmouth, Dennis Sciama Building, Portsmouth, PO1 3FX, UK
- ⁹School of Mathematics and Physics, University of Queensland, 4072, Australia
- ¹⁰Department of Physics, The University of Texas at Dallas, Richardson, TX 75080, USA
- ¹¹Departamento de Física, Universidad de Guanajuato - DCI, C.P. 37150, Leon, Guanajuato, México
- ¹²Instituto Avanzado de Cosmología A. C., San Marcos 11 - Atenas 202. Magdalena Contreras, 10720. Ciudad de México, México
- ¹³Physics Dept., Boston University, 590 Commonwealth Avenue, Boston, MA 02215, USA
- ¹⁴Physics Department, Stanford University, Stanford, CA 93405, USA
- ¹⁵SLAC National Accelerator Laboratory, Menlo Park, CA 94305, USA
- ¹⁶Department of Physics & Astronomy, University College London, Gower Street, London, WC1E 6BT, UK
- ¹⁷Instituto de Física, Universidad Nacional Autónoma de México, Cd. de México C.P. 04510, México
- ¹⁸NSF NOIRLab, 950 N. Cherry Ave., Tucson, AZ 85719, USA
- ¹⁹Department of Physics & Astronomy and Pittsburgh Particle Physics, Astrophysics, and Cosmology Center (PITT PACC), University of Pittsburgh, 3941 O'Hara Street, Pittsburgh, PA 15260, USA
- ²⁰Departamento de Física, Universidad de los Andes, Cra. 1 No. 18A-10, Edificio Ip, CP 111711, Bogotá, Colombia
- ²¹Observatorio Astronómico, Universidad de los Andes, Cra. 1 No. 18A-10, Edificio H, CP 111711 Bogotá, Colombia

- ²²Institut d'Estudis Espacials de Catalunya (IEEC), 08034 Barcelona, Spain
- ²³Institute of Space Sciences, ICE-CSIC, Campus UAB, Carrer de Can Magrans s/n, 08913 Bellaterra, Barcelona, Spain
- ²⁴Center for Cosmology and AstroParticle Physics, The Ohio State University, 191 West Woodruff Avenue, Columbus, OH 43210, USA
- ²⁵Department of Physics, The Ohio State University, 191 West Woodruff Avenue, Columbus, OH 43210, USA
- ²⁶The Ohio State University, Columbus, 43210 OH, USA
- ²⁷Sorbonne Université, CNRS/IN2P3, Laboratoire de Physique Nucléaire et de Hautes Energies (LPNHE), FR-75005 Paris, France
- ²⁸Departament de Física, Serra Hünter, Universitat Autònoma de Barcelona, 08193 Bellaterra (Barcelona), Spain
- ²⁹Institut de Física d'Altes Energies (IFAE), The Barcelona Institute of Science and Technology, Campus UAB, 08193 Bellaterra Barcelona, Spain
- ³⁰Institució Catalana de Recerca i Estudis Avançats, Passeig de Lluís Companys, 23, 08010 Barcelona, Spain
- ³¹Department of Physics and Astronomy, Siena College, 515 Loudon Road, Loudonville, NY 12211, USA
- ³²Department of Physics and Astronomy, University of Waterloo, 200 University Ave W, Waterloo, ON N2L 3G1, Canada
- ³³Perimeter Institute for Theoretical Physics, 31 Caroline St. North, Waterloo, ON N2L 2Y5, Canada
- ³⁴Waterloo Centre for Astrophysics, University of Waterloo, 200 University Ave W, Waterloo, ON N2L 3G1, Canada
- ³⁵Instituto de Astrofísica de Andalucía (CSIC), Glorieta de la Astronomía, s/n, E-18008 Granada, Spain
- ³⁶Department of Physics, Kansas State University, 116 Cardwell Hall, Manhattan, KS 66506, USA
- ³⁷Department of Physics and Astronomy, Sejong University, Seoul, 143-747, Korea
- ³⁸CIEMAT, Avenida Complutense 40, E-28040 Madrid, Spain
- ³⁹Department of Physics, University of Michigan, Ann Arbor, MI 48109, USA
- ⁴⁰University of Michigan, Ann Arbor, MI 48109, USA
- ⁴¹Department of Physics & Astronomy, Ohio University, Athens, OH 45701, USA
- ⁴²National Astronomical Observatories, Chinese Academy of Sciences, A20 Datun Rd., Chaoyang District, Beijing, 100012, P.R. China